# CONFORMAL STRUCTURE OF MINIMAL SURFACES WITH FINITE TOPOLOGY

JACOB BERNSTEIN AND CHRISTINE BREINER

Abstract. In this paper, we show that a complete embedded minimal surface in $\mathbb{R}^3$ with finite topology and one end is conformal to a once-punctured compact Riemann surface. Moreover, using the conformality and embeddedness, we examine the Weierstrass data and conclude that every such surface has Weierstrass data asymptotic to that of the helicoid. More precisely, if $g$ is the stereographic projection of the Gauss map, then in a neighborhood of the puncture, $g(p) = \exp(i\alpha z(p) + F(p))$, where $\alpha \in \mathbb{R}$, $z = x_3 + ix_3^*$ is a holomorphic coordinate defined in this neighborhood and $F(p)$ is holomorphic in the neighborhood and extends over the puncture with a zero there. This further implies that the end is actually Hausdorff close to a helicoid.

## 1. Introduction

We apply the techniques of [1] to study complete embedded minimal surfaces with finite topology and one end. The space $\mathcal{E}(1)$ of such surfaces is non-trivial; the embedded genus one helicoid, $\mathcal{H}$ (see figure 1), constructed in [11] by Hoffman, Weber, and Wolf provides an example which moreover has the property of being asymptotically helicoidal (see also [19] for a good exposition). We note that Colding and Minicozzi, in [8], show that any surface in $\mathcal{E}(1)$ is necessarily properly embedded, a fact we use throughout.

The construction and study of $\mathcal{H}$, as well as objects in the larger class where embeddedness is dropped, has a rich history. Using the Weierstrass representation, Hoffman, Karcher, and Wei in [10] first constructed an immersed genus one helicoid. Computer graphics suggested it was embedded, but the existence of an embedded genus one helicoid (in fact $\mathcal{H}$) followed only after Hoffman and Wei proposed a new construction in [13]. They considered $\mathcal{H}$ as the limit of a family of screw-motion invariant minimal surfaces with periodic handles and a helicoidal end. Weber, Hoffman, and Wolf confirmed the existence of such a family of surfaces in [12] and ultimately proved embeddedness of $\mathcal{H}$ in [11]. Hoffman, Weber, and Wolf conjecture that $\mathcal{H}$ is

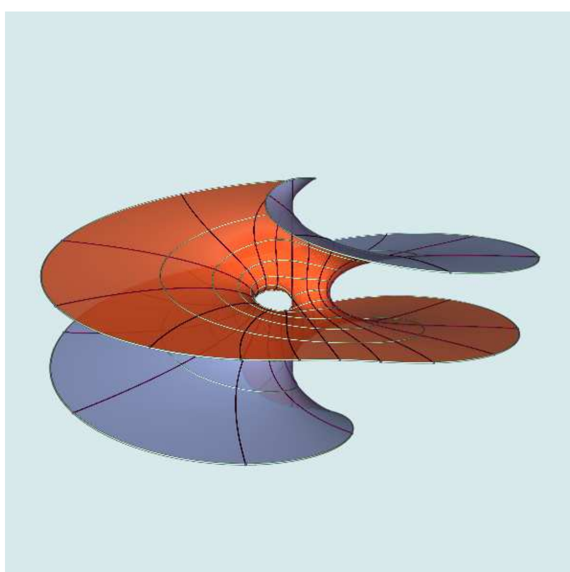

Figure 1. A genus one helicoid (Courtesy of Matthias Weber)

not only the same surface as the one produced in [10], but is actually the unique element of $\mathcal{E}(1)$ with genus one. Recently, Hoffman and White, in [14], used a variational argument to construct an embedded genus one helicoid, though whether their construction is $\mathcal{H}$ is unknown.

In [15], Hoffman and White proved rigidity results for immersed minimal genus one surfaces with one end that in addition contain the $x_1$ and $x_3$-axes. In particular, they showed the surface is conformally a punctured torus with end asymptotic to a helicoid. In this paper, we show that any $\Sigma \in \mathcal{E}(1)$ is conformally a once punctured, compact Riemann surface, with Weierstrass data that has helicoid-like behavior at the puncture. Precisely,

**Theorem 1.1.** *$\Sigma$ is conformally a punctured, compact Riemann surface. Moreover, the height differential, $dh$, extends meromorphically over the puncture with a double pole, as does the meromorphic one form $\frac{dg}{g}$.*

In [16], Meeks and Rosenberg discuss how one might be able to show something similar to Theorem 1.1 for surfaces in $\mathcal{E}(1)$ and the implications this has to the possible conformal structure of complete embedded minimal surfaces in $\mathbb{R}^3$. They do this without going into the details or addressing the difficulties, but indicate how such a statement may be proved using the ideas and techniques of their paper. That is, they anticipated a proof using their derivation of the uniqueness of the helicoid from the lamination result of Colding and Minicozzi [7]. This paper grew out of a desire to give a complete proof of such a result and to use more directly the fundamental work of Colding and Minicozzi in [2, 4, 5, 6, 7].

Theorem 1.1 completes the understanding of the conformal structure of minimal surfaces with finite topology. In [17], Meeks and Rosenberg prove conformality results for properly embedded minimal surfaces of finite topology (i.e. surfaces diffeomorphic to a compact surface with a finite number of punctures) and two or more ends. Using their work, Corollary 0.13 of [8], and Theorem 1.1, we have the following:

**Corollary 1.2.** *Every complete, embedded minimal surface of finite topology in $\mathbb{R}^3$ is conformal to a compact Riemann surface with a finite number of punctures.*

Recall the Weierstrass representation takes a triple $(M, g, dh)$ where $M$ is a Riemann surface, $g$ is a meromorphic function and $dh$ is a meromorphic one form (which has a zero everywhere $g$ has a pole or zero) and gives a minimal immersion in $\mathbb{R}^3$

$$\mathbf{F} := \operatorname{Re} \int \left( \frac{1}{2}(g^{-1} - g), \frac{i}{2}(g^{-1} + g), 1 \right) dh. \tag{1.1}$$

Any immersed minimal surface in $\mathbb{R}^3$ admits such a representation. For the helicoid with $z \in \mathbb{C}$ one has:

$$g := e^{i\alpha z}; \quad dh := dz; \quad \alpha \in \mathbb{R}. \tag{1.2}$$

Notice that on the helicoid both $\frac{dg}{g}$ and $dh$ have double poles at infinity; moreover, $\frac{dg}{g} - i\alpha dh$ is identically zero. For $\Sigma \in \mathcal{E}(1)$, Theorem 1.1, the Weierstrass representation, and embeddedness imply that near the puncture the Weierstrass data is asymptotic to that of a helicoid.

**Corollary 1.3.** *There exists an $\alpha \in \mathbb{R}$ so $\frac{dg}{g} - i\alpha dh$ has holomorphic extension over the puncture, with a zero at the puncture. Equivalently, after possibly translating parallel to the $x_3$-axis, in an appropriately chosen neighborhood of the puncture, $\Gamma$, $g(p) = \exp(i\alpha z(p) + F(p))$ where $F : \Gamma \to \mathbb{C}$ extends holomorphically over the puncture with a zero there and $z = x_3 + i x_3^*$ is a holomorphic coordinate on $\Gamma$. (Here $x_3^*$ is the harmonic conjugate of $x_3$ and is well defined in $\Gamma$.)*

As a consequence of this we may appeal to [9] where the behavior of annular ends with this type of Weierstrass data are studied. In particular, Hauswirth, Perez and Romon show that such an end is $C^0$-asymptotic[1] to a (vertical) helicoid $H$ as long as the data satisfies a certain flux condition. In the present situation, as the data is actually defined on a once punctured compact surface, this condition is automatically satisfied by Stokes' theorem and hence:

**Corollary 1.4.** *If $\Sigma \in \mathcal{E}(1)$ is non-flat then $\Sigma$ is $C^0$-asymptotic to some helicoid.*

[1] i.e. for any $\epsilon > 0$ there exists $R_\epsilon > 0$ so that the part of the end outside of $B_{R_\epsilon}(0)$ has Hausdorff distance to $H$ less than $\epsilon$

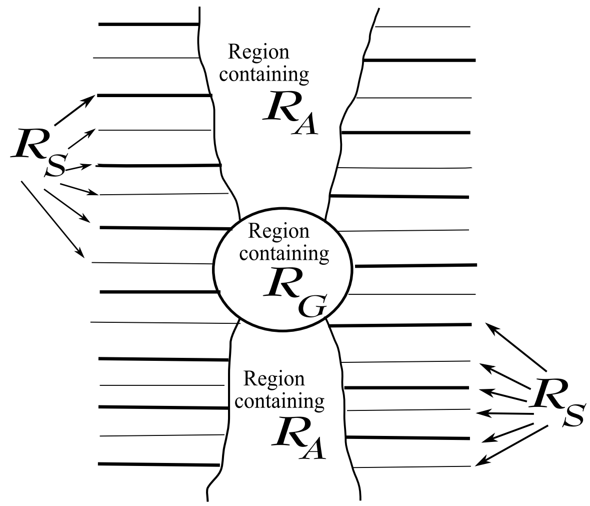


FIGURE 2. A rough sketch of the three regions in the decomposition of $\Sigma$ as outlined in Theorem 1.5.

Let us now recall the argument of [1]. There it is shown that any complete, non-flat, properly embedded minimal disk can be decomposed into two regions: one a region of strict spiraling, i.e. the union of two strictly spiraling multi-valued graphs, and the other a neighborhood of the axis along which the graphs are glued and where the normal is nearly orthogonal to the axis. This follows from existence results for multi-valued minimal graphs in embedded disks found in [5] and an approximation result for such minimal graphs from [3]. The strict spiraling is then used to see that $\nabla_\Sigma x_3 \neq 0$ everywhere on the surface; thus, the Gauss map is not vertical and the holomorphic map $z = x_3 + ix_3^*$ is a holomorphic coordinate. By looking at the log of the stereographic projection of the Gauss map, the strict spiraling is used to show that $z$ is actually a proper map and thus, conformally the surface is the plane. Finally, this gives strong rigidity for the Weierstrass data implying the surface is a helicoid. This result was first shown by Meeks and Rosenberg in [16].

For $\Sigma \in \mathcal{E}(1)$, as there is finite genus the topology of $\Sigma$ is concentrated in a ball in $\mathbb{R}^3$, and so by the maximum principle, all components of the intersection of $\Sigma$ with a ball disjoint from the genus are disks. Hence, outside of a large ball, one may use the local results of [4, 5, 6, 7] about embedded minimal disks. In [1], the trivial topology of $\Sigma$ allows one to deduce global geometric structure immediately from these local results. For $\Sigma \in \mathcal{E}(1)$, the presence of non-zero genus complicates matters. Nevertheless, the global structure will follow from the far reaching description of embedded minimal surfaces given by Colding and Minicozzi in [2]. In particular, as $\Sigma$ has one end, globally it looks like a helicoid (see Appendix B). Following [1], we first prove a sharper description of the global structure (in Section 2.5); indeed, one may generalize the decomposition of [1] to $\Sigma \in \mathcal{E}(1)$ as:

**Theorem 1.5.** *There exist $\epsilon_0 > 0$ and $\mathcal{R}_A$, $\mathcal{R}_S$, and $\mathcal{R}_G$, disjoint subsets of $\Sigma$, such that $\Sigma = \mathcal{R}_A \cup \mathcal{R}_S \cup \mathcal{R}_G$. The set $\mathcal{R}_G$ is compact, connected, has connected boundary and $\Sigma \backslash \mathcal{R}_G$ has genus 0. $\mathcal{R}_S$ can be written as the union of two (oppositely oriented) multi-valued graphs $u^1$ and $u^2$ with $u^i_\theta \neq 0$. Finally, (after a rotation of $\mathbb{R}^3$) $|\nabla_\Sigma x_3| \geq \epsilon_0$ in $\mathcal{R}_A$. (See Figure 2)*

*Remark* 1.6. Here $u^i$ multi-valued means that it can be decomposed into $N$-valued $\epsilon$-sheets (see Definition 2.1) with varying center. The angular derivative, $(u_i)_\theta$, is then with respect to the obvious polar form on each of these sheets. For simplicity we will assume throughout that both $u^i$ are $\infty$-valued.

As an important step in establishing the decomposition theorem, notice that the minimal annulus $\Gamma = \Sigma \backslash \mathcal{R}_G$ has exactly the same weak asymptotic properties as an embedded non-flat minimal disk. Thus, as in [1], strict spiraling in $\mathcal{R}_S$ and a lower bound for $|\nabla_\Sigma x_3|$ on $\mathcal{R}_A$ together give (for appropriately chosen $\mathcal{R}_G$):

**Proposition 1.7.** *In $\Gamma$, $\nabla_\Sigma x_3 \neq 0$ and, for all $c \in \mathbb{R}$, $\Gamma \cap \{x_3 = c\}$ consists of either one smooth, properly embedded curve or two smooth, properly embedded curves each with one endpoint on $\partial\Gamma$.*

The decomposition allows us to argue as in [1], though the non-trivial topology again adds some technical difficulties. By Stokes' Theorem, $x_3^*$ (the harmonic conjugate of $x_3$) exists on $\Gamma$ and thus there is a well defined holomorphic map $z : \Gamma \to \mathbb{C}$ given by $z = x_3 + ix_3^*$. Proposition 1.7 implies that $z$ is a holomorphic coordinate on $\Gamma$. We claim that $z$ is actually a proper map and so $\Gamma$ is conformally a punctured disk. Following [1], this can be shown by studying the Gauss map. On $\Gamma$, the stereographic projection of the Gauss map, $g$, is a holomorphic map that avoids the origin. Moreover, the minimality of $\Sigma$ and the strict spiraling in $\mathcal{R}_S$ imply that the winding number of $g$ around the inner boundary of $\Gamma$ is zero. Hence, by monodromy there exists a holomorphic map $f : \Gamma \to \mathbb{C}$ with $g = e^f$. Then, as in [1], the strict spiraling in $\mathcal{R}_S$ imposes strong control on $f$ which is sufficient to show that $z$ is proper. Further, once we establish $\Gamma$ is conformally a punctured disk, the properties of the level sets of $f$ imply that it extends meromorphically over the puncture with a simple pole. This gives Theorem 1.1 and ultimately Corollaries 1.3 and 1.4.

## 2. Decomposition of $\Sigma$

In the next four subsections, we develop the tools needed to prove the structural results of Theorem 1.5 and Proposition 1.7. Many of these are extensions of those developed for the simply connected case, which can be found in Section 2 of [1]. We prove Theorem 1.5 and Proposition 1.7 at the conclusion of subsection 2.5.

2.1. **Preliminaries.** We first introduce some notation. Throughout the paper, let $\Sigma \in \mathcal{E}(1)$ and have positive genus, i.e. $\Sigma$ is a complete, properly embedded minimal surface with finite and positive genus, $k$, and one end. Here we say that a surface has genus $k$ if it is homeomorphic to a compact genus $k$ Riemann surface with at most a finite number of punctures. As $\Sigma$ has one end and is complete in $\mathbb{R}^3$, there exists an $R > 0$ so that one of the components $\overline{\Sigma}$ of $\Sigma \cap B_R$ is a compact surface with connected boundary and genus $k$. Thus, $\Sigma \backslash \overline{\Sigma}$ has genus 0 and is a neighborhood of the end of $\Sigma$. We now homothetically rescale so that the genus, $\overline{\Sigma}$, lies in $B_1$ and so that $\sup_{\overline{\Sigma}} |A|^2 \geq 1$.

Denote by $\Pi : \mathbb{R}^3 \to \mathbb{R}^2$ the projection $\Pi(x_1, x_2, x_3) = (x_1, x_2)$. Let

$$\mathbf{C}_\delta(y) = \left\{x : (x_3 - y_3)^2 \leq \delta^2\left((x_1 - y_1)^2 + (x_2 - y_2)^2\right)\right\} \subset \mathbb{R}^3 \tag{2.1}$$

be the complement of a cone and set $\mathbf{C}_\delta = \mathbf{C}_\delta(0)$. Given a real-valued function, $u$, defined on a domain $\Omega \subset \mathbb{R}^+ \times \mathbb{R}$, define the map $\Phi_u : \Omega \to \mathbb{R}^3$ by $\Phi_u(\rho, \theta) = (\rho\cos\theta, \rho\sin\theta, u(\rho, \theta))$ so the image is a multi-valued graph. A natural domain is the polar rectangle:

$$S_{r_1,r_2}^{\theta_1,\theta_2} = \{(\rho, \theta) \mid r_1 \leq \rho \leq r_2, \theta_1 \leq \theta \leq \theta_2\}. \tag{2.2}$$

Indeed, for $u$ defined on $S_{r_1,r_2}^{\theta_1,\theta_2}$, $\Phi_u(S_{r_1,r_2}^{\theta_1,\theta_2})$ is a multi-valued graph over the annulus $D_{r_2} \backslash D_{r_1}$. Thus, $\Gamma_u := \Phi_u(\Omega)$ is the graph of $u$, and $\Gamma_u$ is embedded if and only if $w \neq 0$, where the separation $w$ of $u$ is defined as $w(\rho, \theta) = u(\rho, \theta + 2\pi) - u(\rho, \theta)$.

Recall that $u$ satisfies the minimal surface equation if:

$$\operatorname{div}\left(\frac{\nabla u}{\sqrt{1 + |\nabla u|^2}}\right) = 0. \tag{2.3}$$

The multi-valued graphs $u$ of interest will also be shown to satisfy the following flatness condition:

$$|\nabla u| + \rho|\text{Hess}_{\,u}| + 4\rho\frac{|\nabla w|}{|w|} + \rho^2\frac{|\text{Hess}_{\,w}|}{|w|} \leq \epsilon < \frac{1}{2\pi}. \tag{2.4}$$

As multi-valued minimal graphs are fundamental to the description of the asymptotic behavior, we introduce the following normalization at $\infty$:

**Definition 2.1.** A multi-valued minimal graph $\Sigma_0$ is an *$N$-valued* ($\epsilon$-)*sheet* (*centered at 0 on the scale 1*), if $\Sigma_0 = \Gamma_u$ and $u$, defined on $S_{1,\infty}^{-\pi N,\pi N}$, satisfies (2.3), (2.4), $\lim_{\rho\to\infty} \nabla u(\rho, 0) = 0$, and $\Sigma_0 \subset \mathbf{C}_\epsilon$.

As in the papers of Colding and Minicozzi, we are interested in points with large curvature relative to nearby points, as around these points multi-valued graphs form (see [5]). The precise definition is:

**Definition 2.2.** The pair $(y, s)$, $y \in \Sigma$, $s > 0$, is a $(C)$ *blow-up pair* if

$$\sup_{B_s(y)\cap\Sigma} |A|^2 \leq 4|A|^2(y) = 4C^2 s^{-2}. \tag{2.5}$$

2.2. **Structural Results.** To obtain the decomposition of Theorem 1.5 we will need two important structural results which generalize results for disks from [4] and [5] (it should be noted that many of the proofs of these results did not require that the surface be a disk but only that the boundary be connected, a fact used in [2]). The first is the existence of an $N$-valued graph starting near the genus and extending as a graph all the way out. The second result is similar but for a blow-up pair far from the genus. Namely, for such a pair a multi-valued graph forms on the scale of the pair and extends as a graph all the way out. It may be helpful to compare with the comparable results for disks, i.e. Theorem 0.3 of [4] and Theorem 0.4 of [5].

Note that variants of the propositions are used in [2], specifically in the proof of the compactness result, i.e. Theorem 0.9 for finite genus surfaces, though they are not made explicit there. For the sake of completeness we provide proofs (in Appendix B) of these propositions using Theorem 0.9 of [2]. Note that while both propositions require a rotation of $\mathbb{R}^3$, they are the same rotation. This can be seen because we prove both propositions by a compactness argument that appeals to the Colding-Minicozzi lamination theory of [2]. The only rotation needed is the initial rotation required in Theorem 0.9 of [2].

**Proposition 2.3.** *Given $\epsilon > 0$ and $N \in \mathbb{Z}^+$ there exists an $R > 0$ so that: After a rotation of $\mathbb{R}^3$ there exists an $N$-valued graph $\Sigma_g \subset \Sigma$ over the annulus $D_\infty \backslash D_R \subset \{x_3 = 0\}$, with gradient bounded by $\epsilon$ and in $\mathbf{C}_\epsilon$.*

**Proposition 2.4.** *Given $\epsilon > 0$ sufficiently small and $N \in \mathbb{Z}^+$ there exist $C_1, C_2 > 0$ and $R > 0$ so: After a rotation of $\mathbb{R}^3$, if $(y, s)$ is a $C_1$ blow-up pair in $\Sigma$ and $|y| \geq R$ then there exists an $N$-valued graph $\Sigma_g$ over the annulus $D_\infty \backslash D_s(\Pi(y)) \subset \{x_3 = 0\}$ with gradient bounded by $\epsilon$ and in the cone $\mathbf{C}_\epsilon(y)$, with initial separation bounded below by $C_2 s$. Finally, $\mathrm{dist}_\Sigma(\Sigma_g, y) \leq 2s$.*

2.3. **Blow-up Sheets.** In order to get the strict spiraling in the decomposition of Theorem 1.5 we need to check that the multi-valued graphs that make up most of $\Sigma$ can be consistently normalized. To that end, we note that for blow-up pairs far enough from the genus one obtains a nearby $\epsilon$-sheet (i.e. we have a normalized multi-valued graph). Indeed, the proof of Theorem 7.1 of [1] applies without change to blow-up pairs satisfying the conditions of Proposition 2.4. We claim that in between this sheet, $\Sigma$ consists of exactly one other $\epsilon$-sheet.

**Theorem 2.5.** *Given $\epsilon > 0$ sufficiently small there exist $C_1, C_2 > 0$ and $R > 1$ so: Suppose $(y, s)$ is a $C_1$ blow-up pair, with $|y| > R$. Then there exist two 4-valued $\epsilon$-sheets $\Sigma_i = \Gamma_{u_i}$ $(i = 1, 2)$ on the scale $s$ centered at $y$ which spiral together (i.e. $u_1(s, 0) < u_2(s, 0) < u_1(s, 2\pi)$). Moreover, the separation over $\partial D_s(\Pi(y))$ of $\Sigma_i$ is bounded below by $C_2 s$.*

*Remark* 2.6. We refer to $\Sigma_1, \Sigma_2$ as ($\epsilon$-)blow-up sheets *associated with* $(y, s)$.

*Proof.* We fix a $\delta > 0$ and note that Lemma B.1 gives a $R > 1$ so that if $|y| > R$ then $y \notin \mathbf{C}_\delta$ and using this $\delta$ and $\epsilon$ we pick $\delta_0 < \epsilon$ as in Corollary C.1 (and increase $R$ if needed). Then, Theorem 7.1 of [1] and Proposition 2.4 together give one $\delta_0$-sheet, $\Sigma_1$, forming near $(y, s)$ for appropriately chosen $C_1$ (and possibly after again increasing $R$). Now as long as the part of $\Sigma$ between the sheets of $\Sigma_1$ make up a second minimal graph, the proof of Theorem 2.3 of [1] applies (and provides the correct $C_2$).

We denote by $E$ the region in $\mathbb{R}^3$ between the sheets of $\Sigma_1$ (see Theorem I.0.10 of [7] or Theorem 2.3 of [1] for a precise definition). Theorem I.0.10 of [7] implies that near the blow-up pair the part of $\Sigma$ between $\Sigma_1$ is a graph $\Sigma_2^{in}$; i.e. if $R_0$ is chosen so $B_{4R_0}(y)$ is disjoint from the genus then $B_{R_0}(y) \cap E \cap \Sigma \backslash \Sigma_1 = \Sigma_2^{in}$. To ensure $\Sigma_{in}^2$ is non-empty, we increase $R$ so that $|y| \geq 8s$ (which we may do by Corollary D.2). On the other hand, Appendix D of that same paper guarantees that, outside of a very large ball centered at the genus, the part of $\Sigma$ between $\Sigma_1$ is a graph, $\Sigma_2^{out}$. That is, for $R_1 \geq |y|$ large, $E \cap \Sigma \backslash (B_{R_1} \cup \Sigma_1) = \Sigma_2^{out}$. Now by one-sided curvature estimates (which Corollary C.1 allows us to use), all the components of $E \backslash \Sigma_1$ are graphs and so it suffices to show that $\Sigma_2^{in}$ and $\Sigma_2^{out}$ are subsets of the same component. Suppose not. Then, as $\Sigma_2^{in}$ is a graph and $\Sigma$ is complete, $\Sigma_2^{in}$ must extend inside $E$ beyond $B_{R_1}$. But this contradicts Appendix D of [7] by giving two components of $\Sigma \backslash \Sigma_1$ in $E \cap \Sigma \backslash B_{R_1}$. □

2.4. **Blow-Up Pairs.** While the properties of $\epsilon$-sheets give the strictly spiraling region of $\Sigma$, to understand the region where these sheets fit together (i.e. the axis), we need a handle on the distribution of the blow-up pairs of $\Sigma$. In the case of trivial topology, non-flatness gives one blow-up pair $(y_0, s_0)$, which in turn yields associated blow-up sheets. Then by Corollary III.3.5 of [6], the blow-up sheets give the existence of nearby

blow-up pairs $(y_{\pm 1}, s_{\pm 1})$ above and below (see also Theorem 2.5 of [1] or Lemma 2.5 of [8]). Iterating, one constructs a sequence of blow-up pairs that give the axis $\mathcal{R}_A$.

Crucially, for the extension of the argument to surfaces in $\mathcal{E}(1)$, the result of [6] is local; it depends only on the topology being trivial in a large ball relative to the scale $s_0$. Thus, the above construction holds in $\Sigma$ as long as one deals with two issues. First, establish the existence of two initial blow-up pairs far from the genus, one above and the other below, with small scale relative to the distance to the genus. Second, show that the iterative process produces blow-up pairs which continue to have small scale (again relative to the distance to the genus).

We claim that the further a blow-up pair is from the genus, the smaller the ratio between the scale and the distance to the genus; hence both issues can be addressed simultaneously. This is an immediate consequence (see Corollary D.2) of the control on curvature around blow-up pairs as given by Proposition D.1 (an extension of Lemma 2.26 of [8] to $\Sigma$). Thus, given an initial blow-up pair far enough above the genus, we can iteratively produce higher and higher blow-up pairs that satisfy the appropriate scale condition, with the same true starting below the genus and going down. Here we establish the existence of a chain of blow-up pairs which will be critical to our decomposition theorem:

**Lemma 2.7.** *Given $\epsilon > 0$ sufficiently small, there exist constants $C_1, C_{in} > 0$ and a sequence $(\tilde{y}_i, \tilde{s}_i)$ of $C_1$ blow-up pairs of $\Sigma$ such that: the sheets associated to $(\tilde{y}_i, \tilde{s}_i)$ are $\epsilon$-sheets on scale $\tilde{s}_i$ centered at $\tilde{y}_i$ and $x_3(\tilde{y}_i) < x_3(\tilde{y}_{i+1})$ for $i \geq 1$, $\tilde{y}_{i+1} \in B_{C_{in}\tilde{s}_i}(\tilde{y}_i)$ while for $i \leq -1$, $\tilde{y}_{i-1} \in B_{C_{in}\tilde{s}_i}(\tilde{y}_i)$.*

*Proof.* Without loss of generality, we work above the genus (i.e. for $x_3 > 1$ and $i \geq 1$), as the argument below the genus is identical. Use $\epsilon$ to choose $C_1, C_2$ and $R$ as in Theorem 2.5. By Corollary III.3.5 of [6] there are constants $C_{out} > C_{in} > 0$ such that, for a $C_1$ blow-up pair $(y, s)$ with $|y| \geq R$, as long as the component of $B_{C_{out}s}(y) \cap \Sigma$ containing $y$ is a disk, we can find blow-up pairs above and below $(y, s)$ and inside $B_{C_{in}s}(y)$. Corollary D.2 and Proposition A.1 ensure a value $h_1 \geq R$, depending on $C_{out}$ so for $|y| \geq h_1$ this condition is satisfied. Thus, it suffices to find an initial blow-up pair $(\tilde{y}_1, \tilde{s}_1)$ with $|\tilde{y}_1| \geq h_1$, as repeated application of Corollary III.3.5 of [6] will give the sequence $(\tilde{y}_i, \tilde{s}_i)$.

Proposition 2.3 and Appendix D of [7] together guarantee the existence of two $\tilde{N}$-valued graphs spiraling together over an unbounded annulus (with inner radius $\overline{R}$). Then, for large enough $\tilde{N}$, the proof of Theorem 2.3 of [1] gives two $N$-valued $\epsilon$-sheets around the genus, $\Sigma_1, \Sigma_2$, on some scale $\tilde{R}$ and in the cone $\mathbf{C}_\epsilon$. Theorem III.3.1 of [6] with $r_0 \geq \max\{1, \tilde{R}, h_1\}$ then implies there is large curvature above and below the genus. Hence, by a standard blow-up argument (see Lemma 5.1 of [5]) one gets the desired $C_1$ blow-up pair $(\tilde{y}_1, \tilde{s}_1)$ above the genus with $|\tilde{y}_1| > 2r_0 \geq h_1$. ☐

2.5. **Decomposing $\Sigma$.** The decomposition of $\Sigma$ now proceeds as in Section 4 of [1], with Proposition 3.3 of [1] giving strict spiraling far enough out in the $\epsilon$-sheets of $\Sigma$. After specifying the region of strict spiraling, $\mathcal{R}_S$, the remainder of $\Sigma$ will be split into the genus, $\mathcal{R}_G$, and the axis, $\mathcal{R}_A$. The strict spiraling, the fact that away from the genus convex sets meet $\Sigma$ in disks (see Lemma A.1) and the proof of Rado's theorem (see [18]) will then give $\nabla_\Sigma x_3 \neq 0$ in $\mathcal{R}_A$. Then a Harnack inequality will allow us to bound $|\nabla_\Sigma x_3|$ from below there.

**Lemma 2.8.** *There exist constants $C_1, R_0, R_1$ and a sequence $(y_i, s_i)$ ($i \neq 0$) of $C_1$ blow-up pairs of $\Sigma$ so that: $x_3(y_i) < x_3(y_{i+1})$ and for $i \geq 1$, $y_{i+1} \in B_{R_1 s_i}(y_i)$ while for $i \leq -1$, $y_{i-1} \in B_{R_1 s_i}(y_i)$. Moreover, if $\mathcal{R}_A = \mathcal{R}_A^+ \cup \mathcal{R}_A^-$ where $\mathcal{R}_A^\pm$ is $\bigcup_{\pm i > 0} \Sigma_{R_1 s_i, y_i}$ (and $\Sigma_{R_1 s_i, y_i}$ is the component of $B_{R_1 s_i}(y_i) \cap \Sigma$ containing $y_i$), then $\mathcal{R}_S = \Sigma \setminus (\mathcal{R}_A \cup B_{R_0})$ has exactly two unbounded components which can be written as the union of two multi-valued graphs $u^1$ and $u^2$, with $u^i_\theta \neq 0$.*

*Proof.* We wish to argue as in Lemma 4.1 of [1] and to do so we must ensure that we may use the chord-arc bounds of [8] and the one-sided curvature estimates of [7] near the pairs $(y_i, s_i)$. As these are both local results it will suffice to work far from the genus.

Fix $\epsilon < \epsilon_0$ where $\epsilon_0$ is given by Proposition 3.3 of [1] which will be important for the strict spiraling. Next pick $\delta > 0$ and apply Corollary C.1 to obtain a $\delta_0 < \epsilon$ and $\tilde{R} > 1$. Now using $\delta_0$ in place of $\epsilon$ let $(\tilde{y}_i, \tilde{s}_i)$ be the sequence constructed in Lemma 2.7. Let us now determine how to choose the $(y_i, s_i)$.

First of all, as long as $y_i \notin \mathbf{C}_\delta \cup B_{\tilde{R}}$ we may use the one-sided curvature estimate in $\mathbf{C}_{\delta_0}(y_i)$. Notice by Lemma B.1 we may increase $\tilde{R}$ and require only that $y_i \notin B_{\tilde{R}}$. Now recall that the chord-arc bounds give a

constant $C_{arc} > 0$ so for any $\gamma > 1$, if the component of $B_{2C_{arc}\gamma s_i}(y_i) \cap \Sigma$ containing $y_i$ is a disk, then the intrinsic ball of radius $C_{arc}\gamma s_i$ centered at $y_i$ contains $B_{\gamma s_i}(y_i) \cap \Sigma$. On $(y_i, s_i)$, we want a uniform bound, $N$, on the number of sheets between the blow-up sheets associated to the pairs $(y_i, s_i)$ and $(y_{i+1}, s_{i+1})$. This is equivalent to a uniform area bound which in turn follows from the chord-arc bounds described above and curvature bounds of Proposition D.1 (for details see Proposition 7.3 of [1]). To correctly apply this argument, one must be sufficiently far from the genus; i.e. for a fixed constant $C_{bnd}$, the component of $B_{C_{bnd}s_i}(y_i) \cap \Sigma$ containing $y_i$ must be a disk. To that end, pick $h_2 \geq 0$ by using Corollary D.2 with $\alpha^{-1} \geq \max\left\{C_{bnd}, 2R_1, \tilde{R}\right\}$ where $R_1$ is to be chosen later. We then pick the sequence $(y_i, s_i)$ from $(\tilde{y}_i, \tilde{s}_i)$ by requiring $x_3(y_i) \geq h_2$ (and then relabelling). Notice that the way we choose the $(y_i, s_i)$ ensures that $N$ is independent of our ultimate choice of $R_1$.

We now determine $R_1$. By choice of $(y_i, s_i)$, the one-sided curvature bounds hold and so there is an $R_2$ such that in $\mathbf{C}_{\delta_0}(y_1)$ all of the (at most) $N$ sheets between the blow-up sheets associated to $(y_1, s_1)$ and $(y_2, s_2)$ are $\delta_0$-sheets on scale $R_2 s_1$ centered on the line $\ell$ which goes through $y_1$ and is parallel to the $x_3$-axis (see Theorem 7.2 of [1]). Label these pairs of $\delta_0$-sheets $\Sigma_k^j$, $k = 1, 2$ and $1 \leq j \leq N$. Proceeding now as in the second paragraph of the proof of Lemma 4.1 in [1], we use $N$, $C_2$ and (2.4) to get $\tilde{C}_2$ so $\tilde{C}_2 s_1$ is a lower bound on the separation of each $\Sigma_k^j$ over the circle $\partial D_{R_2 s_1}(\Pi(y_1)) \subset \{x_3 = 0\}$. Theorem 3.3 of [1] gives a $C_3$, depending on $\tilde{C}_2$, such that outside of a cylinder centered at $\ell$ of radius $R_2 C_3 s_1$, all the $\Sigma_k^j$ strictly spiral. Choose $\tilde{R}_1$, depending only on $C_{in}, N, \delta_0, C_3$ and $R_2$, so $B_{\tilde{R}_1 s_1}(y_1)$ contains this cylinder, the point $y_2$ and meets each $\Sigma_k^j$. Then if $R_1 = C_{arc}\tilde{R}_1$ the preceding is also true of the component of $B_{R_1 s_1}(y_1) \cap \Sigma$ containing $y_1$. By the scaling invariance of strict spiraling and the uniformity of the choices, the same is true for each $(y_i, s_i)$.

Finally, by properness, there exists a finite number, $M$, of $\epsilon$-sheets between the blow-up sheets associated to $(y_{\pm 1}, s_{\pm 1})$. Pick $R_0$ large enough so that outside of the ball of radius $R_0$ the $M$ sheets between the blow-up sheets associated to $(y_1, s_1)$ and $(y_{-1}, s_{-1})$ strictly spiral. Such an $R_0$ exists by Proposition 2.3 and the above argument. □

*Proof.* (Proposition 1.7) By properness there exists an $R_0' \geq R_0$ so that the component of $B_{R_0'} \cap \Sigma$ containing $\overline{\Sigma}$ contains $B_{R_0} \cap \Sigma$. We take $\mathcal{R}_G$ to be this component and note that $\partial \mathcal{R}_G$ is connected by Proposition A.1. The strict spiraling in $\mathcal{R}_S$ and the proof of Rado's theorem gives Proposition 1.7. □

*Proof.* (Theorem 1.5) By using Lemma 2.8 (and making the obvious modifications needed to account for $\mathcal{R}_G$) the proof of Theorem 1.1 of [1] then gives Theorem 1.5 of this paper. □

## 3. Conformal Structure of $\Gamma$

In this section we prove Theorem 1.1 and Corollary 1.3 (in subsection 3.3) by analysis similar to that in Section 5 of [1]. To do so, we first show that $\Gamma = \Sigma \backslash \mathcal{R}_G$ is conformally a punctured disk and, indeed, the map $z = x_3 + i x_3^* : \Gamma \to \mathbb{C}$ is a proper, holomorphic coordinate (here $x_3^*$ is the harmonic conjugate of $x_3$). Note that by Proposition 1.7, as long as $z$ is well defined, it is injective and a conformal diffeomorphism. Thus, it suffices to check that $z$ is well defined and that it is proper; i.e. if $p \to \infty$ in $\Gamma$ then $z(p) \to \infty$.

**Proposition 3.1.** *$x_3^*$ is well defined on $\Gamma$.*

*Proof.* As $\Sigma$ is minimal, ${}^*dx_3$, the conjugate differential to $dx_3$, exists on $\Sigma$ and is closed and harmonic. We wish to show it is exact on $\Gamma$. To do so, it suffices to show that for every closed curve $\nu$ in $\Gamma$, we have $\int_\nu {}^*dx_3 = 0$. By Proposition A.1, $\Sigma \backslash \nu$ has two components, only one of which is bounded. The bounded component, together with $\nu$, is a manifold with (connected) boundary, and on this manifold ${}^*dx_3$ is a closed form. Hence, the result follows immediately from Stokes' theorem. □

3.1. **Existence of $f$.** We now show that there exists $f : \Gamma \to \mathbb{C}$ such that $g = e^f$ on $\Gamma$, where $g$ is the stereographic projection of the Gauss map of $\Sigma$. We argue as in Section 5 of [1], though we must first check that there is a well defined notion of $\log g$ in $\Gamma$. Since $g$ is meromorphic in $\Sigma$ and has no poles or zeros in $\Gamma$, this is equivalent to showing that $g$ has an equal number of poles and zeros.

**Proposition 3.2.** *Counting multiplicity, $g$ has an equal number of poles and zeros.*

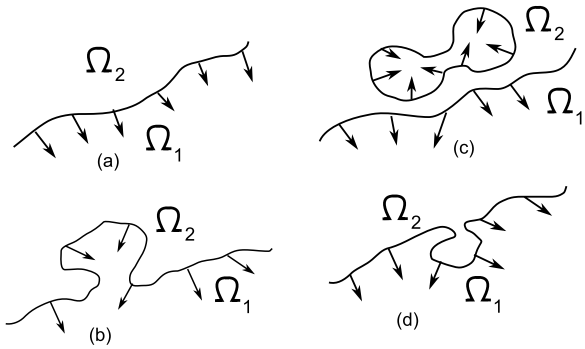


FIGURE 3. Level curve examples in Proposition 3.2. (a) Initial orientation chosen at height $x_3 = h$. (b) A curve pinching off from $\Omega_1$. (c) Two curves pinching from one. (d) A curve pinching off from $\Omega_2$.

*Proof.* The zeros and poles of $g$ occur only at the critical points of $x_3$. In particular, by Proposition 1.7, there exist $h$ and $R$ so that all the zeros and poles are found in the cylinder:

$$C_{h,R} = \left\{|x_3| \leq h, x_1^2 + x_2^2 \leq R^2\right\} \cap \Sigma. \tag{3.1}$$

Moreover, for $R$ and $h$ sufficiently large, $\gamma = \partial C_{h,R}$ is the union of four smooth curves, two at the top and bottom, $\gamma_t$ and $\gamma_b$, and two disjoint helix like curves $\gamma_1, \gamma_2 \subset \mathcal{R}_S$. Hence, for $c \in (-h, h)$, $\{x_3 = c\}$ meets $\partial C_{h,R}$ in exactly two points. Additionally, as $\gamma_1$ and $\gamma_2$ are compact, there is a constant $\alpha > 0$ so $|\frac{d}{dt} x_3(\gamma_i(t))| > \alpha$, $i = 1, 2$.

Let us first suppose that $g$ has only simple zeros and poles and these occur at distinct values of $x_3$, thus, the Weierstrass representation implies that the critical points of $x_3$ are non-degenerate. We now investigate the level sets $\{x_3 = c\}$. By the strict spiraling of $\gamma_i$ ($i = 1, 2$), at the regular values these level sets consist of an interval with end points in $\gamma_i$ ($i = 1, 2$) and the union of a finite number of closed curves. Moreover, by the minimality of $C_{h,R}$, the non-smooth components of the level sets at critical values will consist of either two closed curves meeting in a single point or the interval and a closed curve meeting in a single point. As a consequence of this $\left\{|x_3| \leq h, x_1^2 + x_2^2 \leq R^2\right\} \backslash C_{h,R}$ has exactly two connected components $\Omega_1$ and $\Omega_2$. Orient $C_{h,R}$ by demanding that the normal point into $\Omega_1$. Notice that it is well defined to say if a closed curve appearing in $\{x_3 = c\} \cap C_{h,R}$ surrounds $\Omega_1$ or $\Omega_2$.

The restrictions imposed on $g$ and minimality of $C_{h,R}$ imply that at any critical level, as one goes downward, either a single closed curve is "created" or is "destroyed". (See Figure 3.) Moreover, when such a curve is created it makes sense to say whether it surrounds $\Omega_1$ or $\Omega_2$ and this is preserved as one goes downward. Now suppose a closed curve is created and that it surrounds $\Omega_1$; then it is not hard to see that at the critical point the normal must point upwards. Similarly, if a closed curve surrounding $\Omega_1$ is destroyed then the normal at the critical point is downward pointing. For, closed curves surrounding $\Omega_2$ the opposite is true; i.e. when a closed curve is created then at the critical point the normal points downward. Thus, since the level sets at $h$ and $-h$ are intervals, one sees that the normal points up as much as it points down. That is, $g$ has as many zeros as poles.

We now drop the restrictions on the poles and zeros of $g$. Beyond these assumptions the argument above used only that $C_{h,R}$ was minimal and that the boundary curves $\gamma_i$ ($i = 1, 2$) meet the level curves of $x_3$ in precisely one point. It is not hard to check that these last two conditions are preserved by small rotations around lines in the $x_1$-$x_2$ plane. We claim that such rotations also ensure that the Gauss map of the new surface must have simple poles or zeros and these are on distinct level sets. To that end we let $C^\epsilon_{h,R}$ be the rotation of $C_{h,R}$ by $\epsilon$ degrees around a fixed line $\ell$ in the $x_1$-$x_2$ plane and through the origin (note we do not rotate the ambient $\mathbb{R}^3$). Denote by $\Phi_\epsilon$ the induced isometric isomorphism between the sets.

The strict spiraling of $\gamma_1, \gamma_2$ implies there exists an $\epsilon_0 > 0$, depending on $\alpha$ and $R$ and a constant $K > 0$, depending on $R$ so: for all $0 < \epsilon < \epsilon_0$, if $c \in (-h + K\epsilon, h - K\epsilon)$ then $\{x_3 = c\} \cap C^\epsilon_{h,R}$ meets $\partial C^\epsilon_{h,R}$ in two points. Moreover, by a suitable choice of $\ell$ the critical points will be on distinct level sets. Denote by $g_\epsilon$ the stereographic projection of the Gauss map of $C^\epsilon_{h,R}$. We now use the fact that $g$ is meromorphic on

$\Sigma$ (and thus the zeros and poles of $g$ are isolated) and that $g_\epsilon$ is obtained from $g$ by a Möbius transform. Indeed, these two facts imply that (after shrinking $\epsilon_0$) for $\epsilon \in (0, \epsilon_0)$, $g_\epsilon$ has only simple zeros and poles on $C_{h,R}^\epsilon$ and by our choice of $\ell$ these are on distinct levels of $x_3$. By further shrinking $\epsilon_0$ one can ensure that all of the critical values occur in the range $(-h + K\epsilon, h - K\epsilon)$. Thus, the level sets in $C_{h,R}^\epsilon$ of $x_3$ for $c \in (-h + K\epsilon, h - K\epsilon)$ consist of an interval with endpoints in $\partial C_{h,R}^\epsilon$, one in each $\gamma_i$ for $i = 1, 2$, and the union of a finite number of closed curves.

Our original argument then immediately implies that $g_\epsilon$ has as many zeros as poles. Thus, $\int_{\partial C_{h,R}} \Phi_\epsilon^* \frac{dg_\epsilon}{g_\epsilon} = \int_{\partial C_{h,R}^\epsilon} \frac{dg_\epsilon}{g_\epsilon} = 0$ for $\epsilon < \epsilon_0$. Hence, as $\Phi_\epsilon^* \frac{dg_\epsilon}{g_\epsilon}$ is continuous in $\epsilon$, $\int_{\partial C_{h,R}} \frac{dg}{g} = 0$. □

**Corollary 3.3.** *A holomorphic function $f : \Gamma \to \mathbb{C}$ exists so $e^f = g$ on $\Gamma$.*

3.2. **Concluding properness of $z$.** The strict spiraling in $\mathcal{R}_S$ was used in [1] to show that the map $f = f_1 + i f_2$ was, away from a neighborhood of the axis, a proper conformal diffeomorphism onto the union of two disjoint closed half-spaces. Since every level set of $x_3$ has an end in each of these sets, properness of $z$ was then a consequence of Schwarz reflection and the Liouville theorem. The same is true when there is non-zero genus:

**Proposition 3.4.** *There exists a $\gamma_0 > 0$ so: with $\Omega_\pm = \{x \in \Gamma : \pm f_1(x) \geq \gamma_0\}$, $f$ is a proper conformal diffeomorphism from $\Omega_\pm$ onto $\{z : \pm \mathrm{Re}\, z \geq \gamma_0\}$.*

*Proof.* Pick $\gamma_0$ as in Proposition 5.1 of [1] (where $\gamma_0$ depends only on the $\epsilon_0$ of Theorem 1.5), as long as $f_1^{-1}(\gamma_0) \cap \partial\Gamma = \emptyset$ the proof in [1] carries over unchanged. Note, the proof only depends on having a lower bound for $\gamma_0$ and so we may increase (if necessary) so $\gamma_0 > \max_{\partial \mathcal{R}_G} |f_1|$. □

3.3. **The proofs of Theorem 1.1 and Corollary 1.3.**

*Proof.* (Theorem 1.1) Coupled with the above results, the proof of Proposition 5.2 of [1] then gives that $z \to \pm\infty$ along each level set of $x_3$; that is $z : \Gamma \to \mathbb{C}$ is a proper holomorphic coordinate. Thus, $z(\Gamma)$ contains $\mathbb{C}$ with a closed disk removed; in particular, $\Gamma$ is conformally a punctured disk. Then, since $f_1^{-1}(\gamma_0) \cap \Gamma$ is a single smooth curve, $f$ has a simple pole at the puncture. Similarly, by Proposition 1.7, $z$ has a simple pole at the puncture. In $\Gamma$, the height differential $dh = dz$ and $\frac{dg}{g} = df$. □

Embeddedness and the Weierstrass representation, (1.1), then imply Corollary 1.3:

*Proof.* Theorem 1.1 gives that, in $\Gamma$, $f(p) = \alpha z(p) + \beta + F(p)$ where $\alpha, \beta \in \mathbb{C}$ and $F : \Gamma \to \mathbb{C}$ is holomorphic and has holomorphic extension to the puncture (and has a zero there). By translating $\Sigma$ parallel to the $x_3$-axis and re-basing $x_3^*$ we may assume $\beta = 0$. By Proposition 1.7, $\{x_3 = 0\} \cap \Gamma$ can be written as the union of two smooth proper curves, $\sigma^\pm$, each with one end in $\partial\Gamma$, and parametrized so $x_3^*(\sigma^\pm(t)) = t$ for $\pm t > T$; here $T > 0$ is large enough that $\sigma^\pm(t) \subset \mathcal{R}_S$. Let us denote by $\rho^\pm(t)$ and $\theta^\pm(t)$ the polar coordinates of $\sigma^\pm(t)$. Notice that as we are in $\Gamma$, $\mathrm{Im}\, f(\sigma^\pm(t)) = (\mathrm{Re}\, \alpha) t + \mathrm{Im}\, F(\sigma^\pm(t))$. By the strict spiraling in $\mathcal{R}_S$, there are integers $N^\pm$ so $|\theta^\pm(t) - \mathrm{Im} f(\sigma^\pm(t))| < \pi N^\pm$ (see the proof of Proposition 5.1 of [1]). Thus, since $F(\sigma^\pm(t)) \to 0$ as $|t| \to \infty$, if $\mathrm{Re}\, \alpha \neq 0$ then $\theta^\pm(t)$ is unbounded as $|t|$ increases. That is, $\sigma^+$ and $\sigma^-$ spiral infinitely and in opposite directions. Moreover, the strict spiraling also gives that $\rho^\pm(t)$ is strictly increasing in $|t|$. To see this note that since $\rho'(t) u_\rho(\rho(t), \theta(t)) + \theta'(t) u_\theta(\rho(t), \theta(t)) = 0$ along $\sigma^\pm(t)$ and $u_\theta \neq 0$, $\rho'(t)$ can only vanish when $\theta'(t)$ does. But, our choice of parametrization rules out the simultaneous vanishing of these two derivatives. This contradicts embeddedness, as such curves must eventually intersect. This last fact is most easily seen by looking at the universal cover of the annulus $\{\max\{\rho^\pm(\pm T_0)\} \leq \rho \leq \min\{\rho^\pm(\pm(T_0 + T_1))\}\}$ where $T_0, T_1 > T > 0$ are chosen so $|\theta^\pm(\pm(T_0 + T_1)) - \theta^\pm(\pm T_0)| \geq 4\pi$ and the annulus is non-empty. In particular, by appropriately lifting $\sigma_+$ and $\sigma_-$, the intersection is immediate. Therefore, $\mathrm{Re}\, \alpha = 0$. □

## Appendix A. Topological structure of $\Sigma$

An elementary but crucial consequence of the maximum principle is that each component of the intersection of a minimal disk with a closed ball is a disk. Similarly, each component of the intersection of a genus $k$ surface with a ball has genus at most $k$ (see Appendix C of [7] and Section I of [6]). We note that for $\Sigma$ with one end and finite genus we obtain a bit more:

**Proposition A.1.** *Suppose $\Sigma \in \mathcal{E}(1)$ and $\overline{\Sigma} \subset \Sigma \cap B_1$ is connected and has the same genus as $\Sigma$. Then, $\Sigma \backslash \overline{\Sigma}$ is an annulus. Moreover, for any convex set $C$ with non-empty interior, if $C \cap B_1 = \emptyset$, then each component of $C \cap \Sigma$ is a disk. Alternatively, if $B_1 \subset C$ then all the components of $C \cap \Sigma$ not containing $\overline{\Sigma}$ are disks.*

*Proof.* That $\Sigma \backslash \overline{\Sigma}$ is an annulus is a purely topological consequence of $\Sigma$ having one end. Namely, if $\partial \overline{\Sigma}$ had more than one connected component, the genus of $\Sigma$ would be strictly greater than the genus of $\overline{\Sigma}$.

If $C$ and $B_1$ are disjoint then, as they are convex, there exists a plane $P$ so that $P$ meets $\Sigma$ transversely and so that $P$ separates $B_1$ and $C$. Since $\Sigma \backslash \overline{\Sigma}$ is an annulus and $P \cap \overline{\Sigma} = \emptyset$, the convex hull property implies that $P \cap \Sigma$ consists only of unbounded smooth proper curves. Thus exactly one of the components of $\Sigma \backslash (P \cap \Sigma)$ is not a disk. As $C$ is disjoint from the non-disk component we have the desired result. On the other hand, if $C$ is convex and contains $B_1$, denote by $C'$ the component of $C \cap \Sigma$ containing $\overline{\Sigma}$. Suppose there was a component of $C \cap \Sigma$ not equal to $C'$ that was not a disk, then there would be a subset of $\Sigma$ with boundary in $\bar{C}$ but interior disjoint from $C$, violating the convex hull property. □

## Appendix B. Proofs of Proposition 2.3 and 2.4

We note that Theorem 1.5 is a sharpening, for $\Sigma \in \mathcal{E}(1)$, of a much more general description of the shapes of minimal surfaces given by Colding and Minicozzi in [2]. More precisely, in that paper they show, for a large class of embedded minimal surfaces in $\mathbb{R}^3$, how the geometric structure of a surface is determined by its topological properties. In particular, as $\Sigma$ has finite topology and one end, their work shows that it roughly looks like a helicoid. That is, away from a compact set containing the genus, $\Sigma$ is made up of two infinite-valued graphs that spiral together and are glued along an axis. While we do not make direct use of this description, it is needed in order to derive the structural results of Section 2.2 from the compactness theory of [2]. Thus, we briefly sketch a proof.

First, Theorem A.1 implies that the sequences $\lambda_i \Sigma$, $\lambda_i \to 0$, of homothetic scalings of $\Sigma$ are all uniformly locally simply connected (ULSC); i.e. there is no concentration of topology other than the genus shrinking to a point (see (1.1) of [2] for the rigorous definition). Theorem 0.9 of [2] (particularly its extension to finite genus ULSC surfaces) gives a compactness result for such sequences. Namely, any ULSC sequence of fixed, finite genus surfaces, with boundaries going to $\infty$ and curvature blowing up in a compact set, has a subsequence converging to a foliation, $\mathcal{L}$, of flat parallel planes with at most two singular lines (where the curvature blows up), $\mathcal{S}_1, \mathcal{S}_2$ orthogonal to the leaves of the foliation. Up to a rotation of $\mathbb{R}^3$ we have $\mathcal{L} = \{x_3 = t\}_{t \in \mathbb{R}}$ and so $\mathcal{S}_i$ are parallel to the $x_3$-axis. Away from the singular lines the convergence is in the sense of graphs, in the $C^\alpha$ topology on compact sets for any $0 < \alpha < 1$. Moreover, as explained in property $(C_{ulsc})$ of Theorem 0.9 (see also Proposition 1.5 of [2]), in a small ball centered at a point of the singular set the convergence is (away from the singular set) as a double spiral staircase. We note that in our case, i.e. $\lambda_i \Sigma, \lambda_i \to 0$, there is only one singular line and indeed since $\overline{\Sigma} \subset B_1$ has non-zero curvature this singular line is the $x_3$-axis. To see this, we use a further description of the convergence given by property $(C_{ulsc})$, namely, when there are two singular lines, the double spirals that form around each singular line are glued so that graphs going around both singular lines close up. To be precise, consider bounded, non-simply connected subsets of $\mathbb{R}^3 \backslash (\mathcal{S}_1 \cup \mathcal{S}_2)$ that contain no closed curves homotopic (in $\mathbb{R}^3 \backslash (\mathcal{S}_1 \cup \mathcal{S}_2)$) to a curve around only $\mathcal{S}_i$. That is, consider bounded regions that go only around both singular lines. In these regions, the convergence is as a single valued graph. If this were true of the convergence of $\lambda_i \Sigma$, then one could remove from $\Sigma$ a closed curve disjoint from $\overline{\Sigma}$ and obtain two unbounded components, contradicting that $\Sigma$ has one end. Thus, the local picture near $\mathcal{S}_1$ of a double spiral staircase extends outward and $\Sigma$ has the claimed structure.

The geometric nature of the proof of Theorem 0.9 of [2] implies that $\lambda_i \Sigma$ always converges to the same lamination independent of the choice of $\lambda_i$. We now use the nature of this convergence, that any sequence of homothetic rescalings $\lambda_i \Sigma$, with $\lambda_i \to 0$, has a subsequence that converges to the foliation $\mathcal{L}$ with singular set $\mathcal{S}$, the $x_3$-axis, to deduce gradient bounds in a cone. This and further application of the compactness theory will then give Propositions 2.3 and 2.4.

**Lemma B.1.** *For any $\epsilon > 0, \delta > 0$ there exists an $R > 1$ so every component of $(\mathbf{C}_\delta \backslash B_R) \cap \Sigma$ is a graph over $\{x_3 = 0\}$ with gradient less than $\epsilon$.*

*Proof.* We proceed by contradiction. Suppose there exists a sequence $\{R_i\}$ with $R_i \to \infty$ and points $p_i \in (\mathbf{C}_\delta \backslash B_{R_i}) \cap \Sigma$ such that the component of $B_{\gamma |p_i|}(p_i) \cap \Sigma$ containing $p_i$, $\Omega_i$, is not a graph over $\{x_3 = 0\}$

with gradient less than $\epsilon$. Here $\gamma$ depends on $\delta$ and will be specified later. Now, consider the sequence of rescalings $\frac{1}{|p_i|}\Sigma$, which by possibly passing to a subsequence converges to $\mathcal{L}$. Passing to another subsequence, $\frac{1}{|p_i|}p_i$ converges to a point $p_\infty \in \mathbf{C}_\delta \cap B_1$. Let $\tilde{\Omega}_i = \frac{1}{|p_i|}\Omega_i$. Proposition 1.5 of [2] guarantees that if $B_\gamma(p_\infty) \cap \mathcal{S} = \emptyset$ then the $\tilde{\Omega}_i$ converge to $\tilde{\Omega}_\infty \subset \{x_3 = x_3(p_\infty)\}$ as graphs. As $\mathcal{S}$ is the sole singular set, we may choose $\gamma$ sufficiently small, depending only on $\delta$, to make this happen. Thus, for sufficiently large $j$, $\tilde{\Omega}_j$ is a graph over $\{x_3 = 0\}$ with gradient bounded by $\epsilon$, giving the desired contradiction. □

*Proof.* (Proposition 2.3) Choose $R$ from Lemma B.1 with $\delta = \epsilon$. Note, control on the gradient bounds the separation between sheets. Thus, increasing $R$, if necessary, guarantees $N$ sheets of a graph inside $\mathbf{C}_\epsilon$. □

*Proof.* (Proof of Proposition 2.4) Note that as long as $|y|$ is sufficiently large, Theorem 0.6 of [5] gives an $\Omega < 1/2$ (as well as $C_1$ and $C_2$) so that since the component of $B_{\frac{1}{2}|y|}(y) \cap \Sigma$ containing $y$ is a disk, there exists a $N$-valued graph $\Sigma_0$ over the annulus, $A = D_{\Omega|y|} \backslash D_{s/2}(y) \subset P$ with gradient bounded by $\epsilon/2$, initial separation greater than $C_2 s$ and $\mathrm{dist}_\Sigma(\Sigma_0, y) \leq 2s$. Here $P$ is in principle an arbitrary plane in $\mathbb{R}^3$.

We claim that Lemma B.1 implies a subset, $\Sigma_0'$, of $\Sigma_0$ is a $N$-valued graph over the annulus $A' = D_{\Omega|y|/2} \backslash D_s(\Pi(y)) \subset \{x_3 = 0\}$ with gradient bounded by $\epsilon$, which further implies $\Sigma_0'$ can be extended as desired. To that end we note that for $\delta > 1/(4\Omega)$, if $y \notin \mathbf{C}_\delta$ then $A$ (and thus, by possibly increasing $\delta$, $\Sigma_0$) meets $\mathbf{C}_\delta$. Lemma B.1 allows us to choose an $R_0 > 0$ so that every component of $\Sigma \cap (\mathbf{C}_\delta \backslash B_{R_0})$ is a multi-valued graph over $\{x_3 = 0\}$ with gradient bounded by $\epsilon/4$. Thus if we take $R > 2R_0$ then there is a point of $\Sigma_0$ in $\mathbf{C}_\delta \backslash B_{R_0}$; therefore, for the gradient estimates at the point to be consistent, $P$ must be close enough to $\{x_3 = 0\}$ so that we may choose $\Sigma_0' \subset \Sigma_0$ so it is a multi-valued graph over $A'$. Furthermore, the part of $\Sigma_0'$ over the outer boundary of $A'$ is necessarily inside of $\mathbf{C}_\delta \backslash B_{R_0}$ and so Lemma B.1 allows us to extend it as desired. □

## Appendix C. One-sided Curvature in $\Sigma$

In several places we make use of the one-sided curvature estimate of [7]. Recall that this result gives a curvature estimate for a minimal disk that is close to and on one side of a plane. As a sequence of rescaled catenoids shows, it is crucial that the surface be a disk. In our situation, Proposition A.1 allows the use of the one-sided curvature estimate far from the genus. For convenience we the statement we will need and indicate how it follows from [7]:

**Corollary C.1.** *Given $\epsilon, \delta > 0$ there exist $\delta_0 > 0$ and $R > 1$ such that, if there exists a 2-valued $\delta_0$-sheet on scale $s$ centered at $y$ where $y \notin \mathbf{C}_\delta \cup B_R$, then all the components of $\Sigma \cap (\mathbf{C}_{\delta_0} \backslash B_{2s}(y))$ are multi-valued graphs with gradient $\leq \epsilon$.*

*Proof.* The result follows immediately from the proof of Corollary I.1.9 of [7] as long as one notes that the proof of I.1.9 depends only on each component of $\Sigma \cap \mathbf{C}_{K\delta_0}$ being a disk for $K$ some large (universal) constant. Thus, by Proposition A.1, we need only check that for a suitable choice of $R$ and upper bound $\delta_0'$ for $\delta_0$ (both $R$ and $\delta_0'$ depending only on $\delta$), $y \notin \mathbf{C}_\delta \cup B_R$ implies $\mathbf{C}_{K\delta_0'}(y)$ is disjoint from $B_1$ (i.e. from the genus).

Now suppose $x \in \mathbf{C}_{K\delta_0'}(y)$ and think of $x$ and $y$ as vectors. By choosing $\delta_0'$ sufficiently small (depending on $\delta$) we have that $|\langle x-y, y\rangle| < (1-\gamma)|y||x-y|$ (that is the angle between $x-y$ and $y$ is bounded away from $0°$); note $1 > \gamma > 0$ depends only on $\delta$. But then $|x|^2 = |x-y+y|^2 \geq |x-y|^2 + 2\langle x-y, y\rangle + |y|^2 \geq \gamma |y|^2$. Hence, picking $R^2 > \frac{1}{\gamma}$ suffices. □

## Appendix D. Geometric Bounds Near Blow-up Pairs

We record the following extension of Lemma 2.26 of [8] to surfaces with non-trivial topology. The proof is identical to that of Lemma 2.26 as long as one replaces Colding and Minicozzi's compactness result for minimal disks, i.e. Theorem 0.1 of [7], with the more general Theorem 0.6 of [2]:

**Proposition D.1.** *Given $K_1, g$ we get a constant $K_2$ such that if*

(1) *$\Sigma \subset \mathbb{R}^3$ is an embedded minimal surface with genus$(\Sigma) = g$*
(2) *$\Sigma \subset B_{K_2 s}(y)$ and $\partial\Sigma \subset \partial B_{K_2 s}(y)$*
(3) *$(y, s)$ is a blow-up pair,*

*then we get the curvature bound*

$$\sup_{B_{K_1 s}(y)\cap\Sigma} |A|^2 \leq K_2 s^{-2}. \tag{D.1}$$

An immediate corollary is that, for blow-up pairs far from the genus, the scale is small relative to distance to the genus.

**Corollary D.2.** *Given $\alpha, C_1 > 0$ there exists an $R$ such that for $(y, s)$, a $C_1$ blow-up pair of $\Sigma$ with $|y| \geq R$ then $s < \alpha|y|$.*

*Proof.* Recall we have normalized $\Sigma$ so $\sup_{B_1\cap\Sigma} |A|^2 \geq 1$. Now suppose the result did not hold. Then there exists a sequence $(y_j, s_j)$ of $C_1$ blow-up pairs with $|y_j| \geq j$ and $s_j \geq \alpha|y_j|$. Set $K_1 = 2/\alpha$. By Proposition D.1 there exists $K_2$ such that $\sup_{B_{K_1 s_j}(y_j)\cap\Sigma} |A|^2 \leq K_2 s_j^{-2}$. Since $B_1 \subset B_{K_1 s_j}(y_j)$, $\sup_{B_1\cap\Sigma} |A|^2 \leq K_2 s_j^{-2}$. But $s_j \geq \alpha|y_j| \geq \alpha j$, thus for $j$ sufficiently large one obtains a contradiction. □

## References


1. J. Bernstein and C. Breiner, *Helicoid-like embedded minimal disks*, Preprint. `http://arxiv.org/abs/0802.1497`.
2. T. H. Colding and W. P. Minicozzi II, *The Space of Embedded Minimal Surfaces of Fixed Genus in a 3-manifold V; Fixed Genus*, Preprint.
3. ______, *An excursion into geometric analysis*, Surv. in Diff. Geom. **IX** (2004), 83–146.
4. ______, *The space of embedded minimal surfaces of fixed genus in a 3-manifold I; Estimates off the axis for disks*, Ann. of Math. (2) **160** (2004), no. 1, 27–68.
5. ______, *The space of embedded minimal surfaces of fixed genus in a 3-manifold II; Multi-valued graphs in disks*, Ann. of Math. (2) **160** (2004), no. 1, 69–92.
6. ______, *The space of embedded minimal surfaces of fixed genus in a 3-manifold III; Planar domains*, Ann. of Math. (2) **160** (2004), no. 2, 523–572.
7. ______, *The space of embedded minimal surfaces of fixed genus in a 3-manifold IV; Locally simply connected*, Ann. of Math. (2) **160** (2004), no. 2, 573–615.
8. ______, *The Calabi-Yau conjectures for embedded surfaces*, Ann. of Math. **167** (2008), no. 1, 211–243.
9. L. Hauswirth, J. Perez, and P. Romon, *Embedded minimal ends of finite type*, Trans. AMS **353** (2001), no. 4, 1335–1370.
10. D. Hoffman, H. Karcher, and F. Wei, *Global analysis in modern mathematics*, ch. The Genus One Helicoid and the Minimal Surfaces that Led to its Discovery, Publish or Perish, 1993.
11. D. Hoffman, M. Weber, and M. Wolf, *An embedded genus-one helicoid*, Annals of Math., To Appear.
12. ______, *The genus-one helicoid as a limit of screw-motion invariant helicoids with handles*, Clay Math. Proc., 2, Global theory of minimal surfaces, pp. 243–258.
13. D. Hoffman and F. Wei, *Construction of a helicoid with handle*, Preprint.
14. D. Hoffman and B. White, *Genus-one helicoids from a variational point of view*, Comm. Math. Helv., To Appear.
15. ______, *The geometry of genus-one helicoids*, Comm. Math. Helv., To Appear.
16. W. H. Meeks III and H. Rosenberg, *The uniqueness of the helicoid*, Ann. of Math. (2) **161** (2005), no. 2, 727–758.
17. W.H. Meeks III and H. Rosenberg, *The geometry and conformal structure of properly embedded minimal surfaces of finite topology in $\mathbb{R}^3$*, Invent. Math **114** (1993), no. 3, 625–639.
18. R. Osserman, *A survey of minimal surfaces*, Dover Publications, New York, 1986.
19. M. Weber, D. Hoffman, and M. Wolf, *An embedded genus-one helicoid*, PNAS **102** (2005), no. 46, 16566–16568.